Coordination of *N*-methylpyrrolidone to iron(II)

Keying Ding, Ferdous Zannat, James C. Morris, William W. Brennessel, Patrick L. Holland *

Department of Chemistry, University of Rochester, Rochester, NY 14627, United States

ARTICLE INFO

ABSTRACT

The use of NMP (*N*-methylpyrrolidone) as a cosolvent has been shown to improve the yield of iron-catalyzed cross-coupling reactions, but surprisingly there are no iron complexes of NMP in the literature. This paper reports two novel NMP complexes of iron(II): $Fe_3Cl_6(NMP)_8$ and $L^{tBu}Fe(NMP)Cl$ (L^{tBu} = bulky β-diketiminate ligand). The X-ray crystal structure of $Fe_3Cl_6(NMP)_8$ shows an octahedral $Fe(NMP)_6^{2+}$ cation and two tetrahedral $FeCl_3(NMP)^-$ anions. ^1H NMR spectra show that the NMP ligands are labile, exchanging rapidly on the NMR time scale. The β-diketiminate complex has a trigonal pyramidal geometry with the NMP in an axial position. The use of NMP improves the yield of the catalytic cross-coupling of methyl 4-chlorobenzoate and 1-hexylmagnesium bromide using these and other iron complexes as precatalysts.

1. Introduction

Catalytic cross-coupling reactions are currently dominated by the use of palladium catalysts, which give very high turnover numbers and excellent yields [1]. However, the first cross-coupling catalysts contained less expensive metals like iron, cobalt, and nickel [2,3]. For example, Kochi found that alkenyl halides undergo stereospecific cross-coupling with alkyl Grignard reagents in the presence of catalytic amounts of FeX_3 [3]. In these early reactions, alkenyl halides were used in excess, and substantial amounts of homocoupling were observed.

In more recent years, concerns about the cost and toxicity of palladium and nickel have led chemists to revisit iron catalysts for cross-coupling reactions. Important contributions have come from Fürstner, Cahiez, and Bolm, who have pioneered the renaissance of iron catalysts in these and other catalytic reactions [4,5]. They have shown that simple iron salts are effective precatalysts for cross-coupling reactions. The scope of this reaction is quite broad, and a number of research groups have shown that iron catalysts can form C–C bonds between many substrates with sp^2 and sp^3 carbons, particularly aryls. Interestingly, use of *N*-methylpyrrolidone (NMP) as a cosolvent significantly increases the yield of cross-coupling reactions [6]. For instance, when 1-bromoprop-1-ene was reacted with octylmagnesium chloride in THF with 3% Fe(acac)$_3$, it gave only 40% of 2-undecene. However, when NMP was added as a cosolvent, the yield was 87% [6]. Cahiez et al. proposed that NMP improved the yield by stabilizing the iron-containing active species, preventing decomposition. Although NMP has become a standard additive in these reactions for practical reasons,

there is no direct evidence showing the role of NMP during the catalytic reactions.

NMP has recently been subjected to scrutiny because of its potential toxicity, leading some manufacturers to propose alternatives to NMP [7]. An understanding of the role of NMP in cross-coupling reactions might enable chemists to rationally design alternative additives. A good starting point would be to learn the binding mode, geometry, and lability of NMP in iron complexes. This would help chemists to infer the structural characteristics and behavior of the NMP-containing species that influence the catalytic reactions. In this light, it is surprising that *no iron–NMP complexes have been crystallographically characterized*. In a broader sense, there are only five molecular NMP–transition-metal complexes in the Cambridge Structural Database, containing Y [8,9], Cu [10], and Zn [11,12]. This manuscript describes the first crystallographically verified coordination of NMP to iron, in two complexes. Using these iron(II) compounds, we confirm the beneficial influence of NMP on the yield of a previously characterized catalytic cross-coupling reaction.

2. Results and discussion

2.1. Synthesis, structure, and characterization of $Fe_3Cl_6NMP_8$

When an excess amount of NMP is added to a slurry of $FeCl_2(THF)_{1.5}$ in THF under an atmosphere of argon or N_2, the iron salt dissolves indicating a reaction with the added NMP. This behavior is evident with a variety of stoichiometries from 4 to 100 molar equivalents of NMP to iron. Cooling solutions generated in this way gives light purple crystals that are similar in appearance regardless of the stoichiometry used in the synthesis.

* Corresponding author. Tel.: +1 585 273 3092; fax: +1 585 276 0205.
E-mail address: holland@chem.rochester.edu (P.L. Holland).

The yield of crystals is maximized at 62% when 10 molar equivalents of NMP are used. Elemental analysis of the crystals is consistent with a stoichiometry $FeCl_2(NMP)_{2.6-2.8}$, implying roughly 8 NMP per 3 Fe. The presence of NMP in the crystals is also confirmed using FTIR spectroscopy, which shows a characteristic amide band at 1650 cm^{-1} [13]. This C=O stretching frequency is consistent with the values observed for NMP coordinated to main-group metals such as Ca(II), Mg(II), and Zn(II) [14]. The infrared spectrum also shows a weak C–H band at 2930 cm^{-1}. THF is virtually absent, because the presence of more than 0.3 equiv. of THF per Fe does not agree with the C:N ratio in the elemental analysis (see Scheme 1 and Table 1).

X-ray diffraction elucidates the solid-state structure of the iron–NMP complex. The compound crystallizes in the space group $P\bar{1}$ with one type of iron atom on an inversion center and another type of iron atom on a general position. Therefore there are two distinct iron environments, with twice as many of the latter type of iron atom in the crystal. The overall structure has the empirical formula $Fe_3Cl_6NMP_8$, consistent with the elemental analysis results. The overall Fe:Cl stoichiometry suggests that the iron atoms have retained the ferrous oxidation state (see Table 2).

The less abundant type of iron atom, labeled Fe2, has an octahedral coordination environment with six oxygen atoms from NMP coordinated to the Fe^{2+} ion. In this homoleptic dication $[Fe(NMP)_6]^{2+}$, the O–Fe–O angles between *cis* ligands are between 89.8° and 90.2°, and the *trans* ligands are crystallographically constrained to O–Fe–O angles of 180°. The perspective in Fig. 1 is along the pseudo-S_6 axis relating the NMP ligands, and the individual NMP ligands have very similar metrical parameters.

The more abundant type of iron atom, labeled Fe1, has a tetrahedral coordination environment with one NMP ligand and three
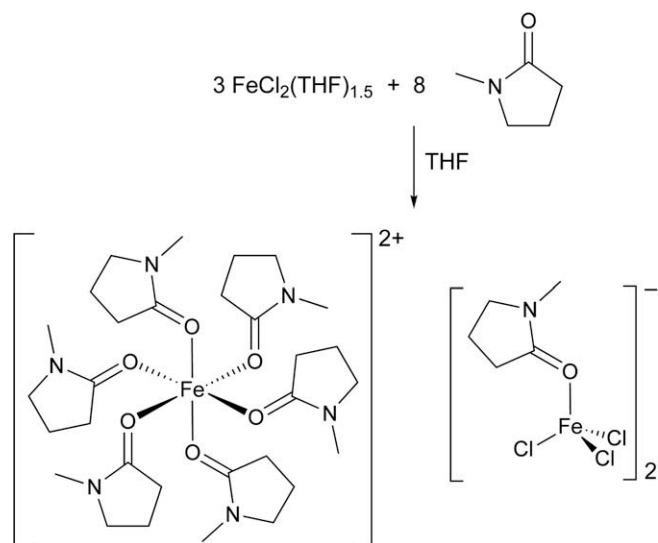
Scheme 1. Synthesis of $Fe_3Cl_6NMP_8$.

Table 1
Important bond distances (Å) and angles (°) in the $Fe(NMP)_6^{2+}$ cation.

Fe2–O2	2.1290(8)
Fe2–O3	2.0998(8)
Fe2–O4	2.1655(8)
O2–Fe2–O3	90.15(3)
O3–Fe2–O4	89.86(3)
O2–Fe2–O4	87.78(3)
Fe2–O2–C6	132.02(8)
Fe2–O3–C11	136.51(8)
Fe2–O4–C16	129.51(8)

Table 2
Important bond distances (Å) and angles (°) in the $FeCl_3(NMP)^-$ anions.

Fe1–O1	2.0553(9)
Fe1–Cl1	2.2858(4)
Fe1–Cl2	2.2959(4)
Fe1–Cl3	2.2921(4)
Cl1–Fe1–O1	102.57(3)
Cl1–Fe1–Cl3	109.131(15)
Cl2–Fe1–Cl3	108.635(15)
Cl2–Fe1–O1	97.36(3)
Fe1–O1–C1	124.46(9)

chloride anions coordinated to the Fe^{2+} ion. These $[FeCl_3NMP]^-$ complex anions are crystallographically equivalent to one another. There is very little variation in the Fe–Cl distances, which range from 2.28 to 2.30 Å. The Fe–O distance in the anions (2.0553(9) Å) is significantly shorter than any of the Fe–O distances in the cation (2.10–2.17 Å): this suggests that the bond-shortening influence of the lower coordination number outweighs the influence of the local charge. Alternatively, this difference could be from the lesser steric pressure of Cl$^-$ as compared to NMP: the latter idea is supported by the smaller Fe–O–C angle of 124.5(1)° in $[FeCl_3NMP]^-$ as compared to the angles of 133(3)° in $[Fe(NMP)_6]^{2+}$.
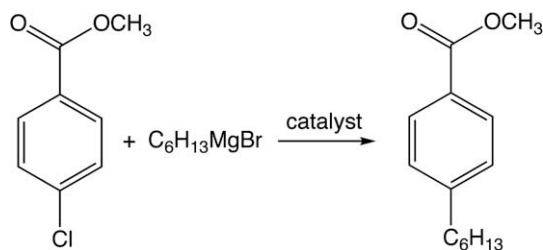
^{1}H NMR spectra of crystals of $Fe_3Cl_6(NMP)_8$ dissolved in THF-d_8 show peaks corresponding to coordinated NMP at δ 9.7, 5.0, 1.9, and −1.4 ppm. The presence of high-spin iron(II) and the magnetic moment of 5.1 μ_B are consistent with the observation of contact-shifted resonances. Importantly, these ^{1}H NMR spectra indicate only one NMP environment at room temperature, even though the X-ray crystal structure shows two different environments for NMP. Cooling the solution to −40 °C in THF-d_8 caused shifting of the peaks, but no apparent splitting due to decoalescence. The observation of a single set of NMP peaks indicates that the NMP ligands are labile in solution, rapidly exchanging between the cationic and anionic iron centers. Our data do not rule out the presence of other rapidly exchanging iron–chloride–NMP species in solution, including $(NMP)_2FeCl_2$ [15].

2.2. Synthesis, structure, and characterization of L^{tBu}FeCl(NMP)

Bulky ligands based on the β-diketiminate template have become popular for stabilizing transition-metal compounds with low coordination numbers at the metal [16]. Numerous iron complexes of the bulky β-diketiminate L^{tBu} (2,2,6,6-tetramethyl-3,5-bis(2,6-diisopropylphenylimido)hept-4-yl) have been characterized [17]. In previous work, we have shown that the three-coordinate complex L^{tBu}FeCl binds neutral donors L to form adducts L^{tBu}Fe(L)Cl, where L = pyridine, acetonitrile, *tert*-butylisonitrile, dimethylformamide, THF, and PPh$_3$ [18,19]. These complexes have an interesting trigonal pyramidal geometry at the iron atom [18]. Therefore, we anticipated that an NMP complex would also be accessible and isolable in this system.

Addition of a slight excess of NMP to a red solution of L^{tBu}FeCl in diethyl ether leads to an immediate color change to yellow-orange. The iron-containing product is isolated in 71% yield as orange crystals that analyzes as L^{tBu}FeCl(NMP) (Scheme 2). Cooling a THF solution gives crystals suitable for X-ray diffraction analysis. The crystals contain four molecules of L^{tBu}FeCl(NMP) per unit cell in addition to unassociated, disordered solvent. The NMP ligand and one isopropyl group are modeled as disordered over two positions each (74:26 and 67:33, respectively), and the major conformer is shown in Fig. 2. Bond lengths and angles are in Table 3.

The Fe–O distance is 2.035(2) Å, slightly less than that in the four-coordinate anions $[FeCl_3NMP]^-$ described above. The Fe–O–C angle of 142.5(3)° is significantly larger than in the cation or anion of $Fe_3Cl_6NMP_8$. Because the diketiminate supporting ligand is

Fig. 1. ORTEP diagram of Fe$_3$Cl$_6$NMP$_8$, using 50% ellipsoids.

Scheme 2. Synthesis of L^{tBu}FeCl(NMP).

Table 3
Important bond distances (Å) and angles (°) in L^{tBu}FeCl(NMP).

Fe–O1	2.035(2)
Fe–Cl	2.2496(6)
Fe–N11	2.0049(13)
Fe–N21	2.0046(13)
N11–Fe–N21	96.9(5)
N11–Fe–Cl	124.61(4)
N21–Fe–Cl	120.95(4)
Cl–Fe–O	106.55(7)
N11–Fe–O	102.56(9)
N21–Fe–O	101.99(9)
Fe–O–C	142.5(3)

pyramidal distortion can be quantified using τ, which has ideal values of $\tau = 1$ for perfect trigonal pyramidal geometry (where the metal sits in the plane of the three basal ligands) and $\tau = 0$ for tetrahedral geometry [21]. The τ value for L^{tBu}Fe(NMP)Cl is 0.35, showing a distinct pyramidal distortion of the iron atom's geometry. The NMP ligand occupies the apical position of the pyramid.

The ^{1}H NMR spectrum of crystals of L^{tBu}FeCl(NMP) dissolved in THF-d_8 shows resonances at δ 18.4, 11.9, 7.3, 5.7, 5.0, 0.4, 0.5, −13.8, and −51.9 ppm. The resonances were broad, preventing integration and the use of the Evans method for determining the solution magnetic susceptibility. However, the structural and spectroscopic similarity to previously characterized high-spin iron(II) complexes L^{tBu}Fe(L)Cl [19] suggests that the new compound is also high-spin iron(II).

2.3. Catalytic cross-coupling reactions with NMP

As described in Section 1, a number of papers have shown that using a mixture of NMP and THF as solvent improves the yield of catalytic cross-coupling reactions relative to the catalytic reaction in THF as the only solvent [4–6]. In order to verify that this trend holds with the compounds discussed here, we performed parallel reactions of methyl 4-chlorobenzoate with hexylmagnesium bromide (Scheme 3) with and without added NMP (roughly 30% v/v). The reactions were allowed to proceed at room temperature under nitrogen for 30 min, quenched with aqueous HCl, and the organic phase was analyzed by comparing the GC response to an internal standard of decane. With 5% loading of iron catalysts, substantial yields of the cross-coupling product methyl 4-hexylbenzoate were detected by GC/MS. In the absence of an iron catalyst, no coupling product was observed.

Fig. 2. ORTEP plot of the major conformer of L^{tBu}FeCl(NMP), using 50% ellipsoids. Disordered solvent is not shown.

much bulkier than the supporting ligands in Fe$_3$Cl$_6$NMP$_8$, this opening of the Fe–O–C angle can be attributed to a steric effect.

The Fe–O distance in L^{tBu}FeCl(NMP) is similar to bonds between iron and other neutral *O*-donors in four-coordinate (diketiminate)iron complexes (2.02 ± 0.14) [20]. Although the geometry at the iron atom is best described as tetrahedral, there is a pyramidal distortion. This distortion has been seen in other iron(II) complexes LFe(X)(L) with neutral σ-donor ligands [18]. The extent of this

Scheme 3. Cross-coupling reaction catalyzed by iron compounds.

Table 4
Yields of catalytic cross-coupling reactions by GC integration, using the conditions specified in Section 4.

Iron catalyst	Yield (THF), %	Yield (THF/NMP), (%)
$FeCl_2(THF)_{1.5}$	30	65
$Fe_3Cl_6(NMP)_8$	53	
$L^{tBu}FeCl$	45	69
$L^{tBu}FeCl(NMP)$	54	
$Fe(acac)_2$	67	75
$Fe(acac)_3$	71	93

The yields of the cross-coupling reactions are shown in Table 4. The most salient comparisons are between the NMP-free compounds and their NMP adducts. For example, $FeCl_2$ (which was used as its THF solvate) [22] gave only 30% yield, but when an excess of NMP was added the yield jumped to 65%. Using a solution of $Fe_3Cl_6NMP_8$ in THF gave 53% yield, and the intermediate value presumably reflects the relatively small amount of NMP present. Comparing the diketiminate complex $L^{tBu}FeCl$, its NMP adduct, and $L^{tBu}FeCl$ in the presence of excess NMP, the yield again increased with larger amounts of NMP. This supports the idea that NMP as a cosolvent, under the conditions used here, is generally useful for improving the yield of catalytic cross-coupling reactions between a Grignard reagent and an aryl halide, as reported by other authors [6,23–32]. Neither of the new compounds here worked as well as the iron acetylacetonate catalyst systems previously described by Cahiez [6].

Bolm and Buchwald recently reported that some iron-catalyzed cross-coupling reactions are greatly influenced by the presence of trace copper impurities [33]. Their experiments showed that 5 ppm copper in some commercial iron chlorides promoted catalysis, and highly purified iron salts did not catalyze the cross-coupling of iodobenzene to form C–N, C–O and C–S bonds. Therefore, there might be some doubt that the catalytic reactions described here come from iron catalysis rather than a small copper impurity. However, the iron(II) precatalysts described here were often purified through crystallization: there was one crystallization in the case of $Fe_3Cl_6NMP_8$, and multiple crystallized intermediates on the synthetic route to $L^{tBu}FeCl(NMP)$. It is unlikely that copper impurities could have persisted through several crystallizations, and even if they did, it is unlikely that the differently purified materials would give similar yields in the catalytic reaction. Therefore, the difficulties from copper impurities previously found for catalysis with simple iron salts [33] are unlikely to be a confounding factor for the particular C—C bonds formed in the reactions described in this work.

3. Conclusions

The reaction of $FeCl_2(THF)_{1.5}$ with NMP formed $Fe_3Cl_6(NMP)_8$. Its X-ray structure showed one octahedral iron center and one tetrahedral iron center in $[Fe(NMP)_6][FeCl_3(NMP)]_2$. Despite the presence of two different iron environments in the solid state, only one environment is evident for the labile NMP ligand from solution [1]H

NMR spectra. NMP also binds to the three-coordinate iron(II) complex $L^{tBu}FeCl$ to give a four-coordinate adduct in which the NMP ligand has similar η^1 binding through the oxygen atom.

The identity of the active iron species in catalytic cross-coupling reactions has not been established. Fürstner has proposed that iron(-II)/magnesium species are important [4], but there is no direct evidence for this species. Although the experiments described here do not address oxidation states other than iron(II), it is now possible to confidently predict that O-coordination of NMP in iron species is reasonable. Finally, we have verified that NMP-coordinated species are more active catalysts than the non-NMP analogues, for several examples of cross-coupling reactions, including a new iron catalyst for the reaction.

4. Experimental

4.1. General considerations

All manipulations were performed in a glove box filled with N_2 or Ar. Glassware was dried at 150 °C overnight. NMR data were recorded on a Bruker Avance 400 spectrometer at 400 MHz, and were referenced to residual THF-d_7 at δ 3.58 and 1.73 ppm. Infrared spectra (1000–4000 cm^{-1}) were recorded on KBr pellet samples in a Shimadzu FTIR spectrophotometer (FTIR-8400S) using 16 scans at 2 cm^{-1} resolution. UV–Vis spectra were measured on a Cary 50 spectrophotometer using screw-cap cuvettes. Elemental analysis was determined by Columbia Analytical Services (Tucson, AZ).

4.2. Synthesis of $Fe_3Cl_6(NMP)_8$

In a glove box filled with N_2, $FeCl_2(THF)_{1.5}$ (250 mg, 1.06 mmol), THF (20 mL), and a stir bar were added to a scintillation vial. N-Methylpyrrolidone (1.0 mL, 11 mmol) was added slowly using a 1 mL syringe. The solution was stirred for 2 h and then filtered through a pad of Celite. The filtrate was kept at −44 °C overnight to yield light purple crystals which were dried under vacuum. The yield was 359 mg (62%). ^{1}H NMR (400 MHz, THF-d_8): δ 9.73 (2H, O=CCH2), 5.01 (3H, N–CH$_3$), 1.86 (2H, C–CH$_2$–C or N–CH$_2$), −1.38 (2H, C–CH$_2$–C or N–CH$_2$) ppm. UV–Vis (THF): 360 (ε = 21 M^{-1} cm^{-1}). IR (KBr pellet): 1650 (s) (C=O), 2930 (w) (C–H) cm^{-1}. Elem. Anal. Calcd. for $Fe_3Cl_6(NMP)_8$: C, 40.95; H, 6.18; N, 9.55. Found: C, 41.04; H, 6.25; N, 9.26%.

4.3. Synthesis of $L^{tBu}FeCl(NMP)$

In a glove box filled with N_2, N-methylpyrrolidone (53 μL, 550 μmol) was added slowly to a solution of $L^{tBu}FeCl$ (312 mg, 526 μmol) [34] in diethyl ether (25 mL). The orange solution was stirred for 2 h and then filtered through Celite. The solution was concentrated to 10 mL and cooled at −35 °C to give pale orange crystals of $L^{tBu}FeCl(NMP)$ (258 mg, 71%). ^{1}H NMR (400 MHz, THF-d_8): δ 18.4, 11.9, 7.3, 5.7, 5.0, 0.4, 0.5, −13.8, −51.9 ppm. UV–Vis (Et$_2$O): 556 (sh) (ε = 230 M^{-1} cm^{-1}); 709 (ε = 430 M^{-1} cm^{-1}). IR (KBr pellet): 1649 (s) (C=O) cm^{-1}, 2931 (m) (C–H) cm^{-1}. Elem. Anal. Calcd. for $L^{tBu}FeCl(NMP)$: C, 69.40; H, 9.03; N, 6.07. Found: C, 68.43; H, 9.43; N, 5.99%. Diketiminate-iron compounds commonly give low carbon analyses, possibly because of the formation of iron carbide.

4.4. Representative procedure for an iron-catalyzed alkyl–aryl cross-coupling reaction

In a nitrogen-filled glove box, a vial was charged with 4-chlorobenzoic acid methyl ester (20.8 mg, 122 μmol), $Fe(acac)_3$ (2.2 mg,

Table 5
Crystallographic parameters.

	$Fe_3Cl_6NMP_8$	$L^{tBu}FeCl(NMP)\cdot$solvent
Empirical formula	$C_{40}H_{72}Cl_6Fe_3N_8O_8$	$C_{40}H_{62}ClFeN_3O$
Formula weight	1173.31	692.23
T (K)	100.0(1)	100.0(1)
Crystal system	Triclinic	Monoclinic
Space group	$P\bar{1}$	$P2_1/n$
Unit cell dimensions		
a (Å)	8.9811(7)	12.5668(15)
b (Å)	10.1907(8)	9.9966(12)
c (Å)	15.0038(12)	34.933(4)
α (°)	84.133(1)	90
β (°)	75.260(1)	96.090(2)
γ (°)	85.025(1)	90
V (Å)	1318.42(18)	4363.7(9)
Z	1	4
D_{Calc} (g/cm^3)	1.478	1.054
Absorption coefficient (mm^{-1})	1.173	0.436
$F(000)$	612	1496
Crystal color, morphology	Pale purple, block	Yellow-orange, block
Crystal size (mm)	$0.23 \times 0.20 \times 0.15$	$0.24 \times 0.16 \times 0.16$
θ range for data collection (°)	2.01–32.03	1.79–31.51
Reflections collected	23 235	71 375
Independent reflections	9045	14 522
Observed reflections	7318	9529
Completeness to theta = 32.03°	98.6%	99.7%
Maximum and minimum transmission	0.8437 and 0.7742	0.9335 and 0.9026
Data/restraints/parameters	9045/0/299	14 522/38/491
Goodness-of-fit on F^2	1.007	1.022
Final R indices [$I > 2\sigma(I)$]	$R_1 = 0.0278$, $wR_2 = 0.0632$	$R_1 = 0.0515$, $wR_2 = 0.1295$
R indices (all data)	$R_1 = 0.0404$, $wR_2 = 0.0684$	$R_1 = 0.0835$, $wR_2 = 0.1421$
Largest difference in peak and hole (e/Å^3)	0.491 and −0.338	0.395 and −0.352

6 μmol), THF (1 mL), decane (0.2 mL) and *N*-methylpyrrolidinone (0.5 mL). A solution of *n*-hexylmagnesium bromide (2 M in Et$_2$O, 0.08 mL, 160 μmol) was added to the solution, causing an immediate color change from red to brown and then dark purple. The resulting mixture was stirred for 25 min, diluted with Et$_2$O, and carefully quenched by the addition of aqueous HCl (0.5 M, ~1 mL). The amount of 4-hexylbenzoic acid methyl ester was quantified by GC–MS analysis of an aliquot from the organic fraction. A new peak with $m/z = 220$ was integrated against decane as internal standard. Standard isolation of 4-hexylbenzoic acid methyl ester includes extraction followed by flash chromatography of the crude product (hexane/ethyl acetate, 30:1), providing the pure product as a colorless oil. Its analytical and spectroscopic data were in excellent agreement with those in the literature [35].

4.5. X-ray crystallography

A crystal was placed onto the tip of a 0.1 mm diameter glass capillary tube or fiber and mounted on a Bruker SMART APEX II CCD Platform diffractometer for a data collection at 100(2) K [36]. The data collection was carried out using Mo Kα radiation (graphite monochromator) with a frame time of 25 (Fe$_3$Cl$_6$NMP$_8$) or 45 (L^{tBu}FeCl(NMP)) seconds and a detector distance of 5 cm. A randomly oriented region of reciprocal space was surveyed: four major sections of frames were collected with 0.50° steps in ω at four different φ settings and a detector position of −33° (Fe$_3$Cl$_6$NMP$_8$) or 38° (L^{tBu}FeCl(NMP)) in 2θ. The intensity data were corrected for absorption [37]. Final cell constants were calculated from the xyz centroids of strong reflections from the actual data collection after integration [38]. See Table 5 for additional crystal and refinement information.

The structure was solved and refined using SHELXL-97 [39]. The space group was determined based on systematic absences and

intensity statistics. A direct-methods solution was calculated which provided most non-hydrogen atoms from the E-map. Full-matrix least squares/difference Fourier cycles were performed which located the remaining non-hydrogen atoms. All non-hydrogen atoms were refined with anisotropic displacement parameters. All hydrogen atoms were placed in ideal positions and refined as riding atoms with relative isotropic displacement parameters. In the structure of L^{tBu}FeCl(NMP), reflection contributions from highly disordred solvent were removed using the SQUEEZE function of PLATON [40], which determined there to be 154 electrons in 683 Å^3 removed per unit cell. In L^{tBu}FeCl(NMP), the NMP ligand was modeled in two orientations, with a ratio of 74:26, and one isopropyl group of the diketiminate ligand was also disordered (67:33).

Appendix A. Supplementary data

Supplementary data associated with this article can be found, in the online version, at doi:10.1016/j.jorganchem.2009.09.005.

References

[1] T. Kohei, N. Miyaura, Top. Curr. Chem. 219 (2002) 1–9.
[2] K. Tamao, T. Hiyama, E. Negishi, J. Organomet. Chem. 653 (2002) 1–4.
[3] M. Tamura, J.K. Kochi, J. Am. Chem. Soc. 93 (1971) 1487–1489.
[4] B.D. Sherry, A. Fürstner, Acc. Chem. Res. 41 (2008) 1500–1511.
[5] A. Correa, O. Garcia Mancheno, C. Bolm, Chem. Soc. Rev. 37 (2008) 1108–1117.
[6] G. Cahiez, H. Avedissian, Synthesis (1998) 1199–1205.
[7] M. Reisch, Chem. Eng. News 86 (2008) 32.
[8] W.J. Evans, C.H. Fujimoto, M.A. Johnston, J.W. Ziller, Organometallics 21 (2002) 1825–1831.
[9] J. Wang, M. Wei, J. Niu, Chin. Sci. Bull. 48 (2003) 2585.
[10] M.R. Churchill, F.J. Rotella, Inorg. Chem. 18 (1979) 853–860.
[11] Q. Zhou, T.W. Hambley, B.J. Kennedy, P.A. Lay, P. Turner, B. Warwick, J.R. Biffin, H.L. Regtop, Inorg. Chem. 39 (2000) 3742–3748.
[12] M.M. Williamson, C.M. Prosser-McCartha, S. Mukundan, C.L. Hill, Inorg. Chem. 27 (1988) 1061–1068.
[13] J.B. Lambert, Introduction to Organic Spectroscopy, Prentice-Hall, New York, 1987.
[14] S.K. Madan, Inorg. Chem. 6 (1967) 421–424.
[15] G. Gritzner, W. Linert, V. Gutmann, J. Inorg. Nucl. Chem. 43 (1981) 1193–1199.
[16] L. Bourget-Merle, M.F. Lappert, J.R. Severn, Chem. Rev. 102 (2002) 3031–3066.
[17] P.L. Holland, Acc. Chem. Res. 41 (2008) 905–914.
[18] J. Vela, J. Cirera, J.M. Smith, R.J. Lachicotte, C.J. Flaschenriem, S. Alvarez, P.L. Holland, Inorg. Chem. 46 (2007) 60–71.
[19] K.P. Chiang, P.M. Barrett, F. Ding, J.M. Smith, S. Kingsley, W.W. Brennessel, M.M. Clark, R.J. Lachicotte, P.L. Holland, Inorg. Chem. 48 (2009) 5106–5116.
[20] F.H. Allen, Acta Crystallogr., Sect. B 58 (2002) 380.
[21] J. Vela, S. Stoian, C.J. Flaschenriem, E. Münck, P.L. Holland, J. Am. Chem. Soc. 126 (2004) 4522–4523.
[22] R.J. Kern, J. Inorg. Nucl. Chem. 24 (1962) 1105–1109.
[23] T. Nagano, T. Hayashi, Org. Lett. 6 (2004) 1297–1299.
[24] M. Nakamura, K. Matsuo, S. Ito, E. Nakamura, J. Am. Chem. Soc. 126 (2004) 3686–3687.
[25] B. Scheiper, M. Bonnekessel, H. Krause, A. Furstner, J. Org. Chem. 69 (2004) 3943–3949.
[26] K. Itami, S. Higashi, M. Mineno, J.-I. Yoshida, Org. Lett. 7 (2005) 1219–1222.
[27] G. Berthon-Gelloz, T. Hayashi, J. Org. Chem. 71 (2006) 8957–8960.
[28] L.K. Ottesen, F. Ek, R. Olsson, Org. Lett. 8 (2006) 1771–1773.
[29] D. Zhang, J.M. Ready, J. Am. Chem. Soc. 128 (2006) 15050–15051.
[30] G. Cahiez, V. Habiak, O. Gager, Org. Lett. 10 (2008) 2389–2392.
[31] A. Fürstner, R. Martin, H. Krause, G. Seidel, R. Goddard, C.W. Lehmann, J. Am. Chem. Soc. 130 (2008) 8773–8787.
[32] P. Le Marquand, G.C. Tsui, J.C.C. Whitney, W. Tam, J. Org. Chem. 73 (2008) 7829–7832.
[33] S.L. Buchwald, C. Bolm, Angew. Chem., Int. Ed. 48 (2009) 5586–5587.
[34] J.M. Smith, R.J. Lachicotte, P.L. Holland, Chem. Commun. (2001) 1542–1543.
[35] J.P. Wolfe, R.A. Singer, B.H. Yang, S.L. Buchwald, J. Am. Chem. Soc. 121 (1999) 9550–9561.
[36] APEX2, version 2.1-0; Bruker AXS, Madison, WI, 2006.
[37] G.M. Sheldrick, SADABS, Version 2007/2, University of Göttingen: Göttingen, Germany, 2004.
[38] SAINT, Version 7.34A, Bruker AXS, Madison, WI, 2006.
[39] SHELXTL, version 6.14, Bruker AXS, Madison, WI, 2000.
[40] A.L. Spek, PLATON, Version 300106, Utrecht University, Utrecht, The Netherlands, 2003.